Polymer Journal, Vol. 36, No. 5, pp. 403—412 (2004)

Solid-State ^{13}C NMR Studies of the Structure and Chain Conformation of Thermotropic Liquid Crystalline Polyether Crystallized from the Liquid Crystalline Glassy Phase

Miwa MURAKAMI, Hiroyuki ISHIDA, Hironori KAJI, and Fumitaka HORII†

Institute for Chemical Research, Kyoto University, Uji, Kyoto 611-0011, Japan

(Received December 22, 2003; Accepted February 17, 2004; Published May 15, 2004)

ABSTRACT: The structure and chain conformation of the form β sample newly crystallized from the liquid crystalline (LC) glassy phase have been investigated for a main-chain thermotropic LC polyether, which was polymerized from 3,3′-dimethyl-4,4′-hydroxyl-biphenyl and 1,10-dibromodecane, by solid-state ^{13}C NMR spectroscopy. The ^{13}C spin–lattice relaxation analyses reveal that there exist two components with different T_{1C} values, which correspond to the crystalline and noncrystalline (supercooled liquid crystalline) components. By employing such differences in T_{1C}, the spectra of the respective components are separately recorded, and the conformations of their CH_2 sequences are evaluated by considering the γ-*gauche* effect on the ^{13}C chemical shifts. As a result, the crystalline component is found to adopt the *t′xxxtxxxt′* conformation whereas another conformation of *t′xxxxxxxt′* is preferably induced in the noncrystalline region, where *t*, *t′*, and *x* indicate *trans*, *trans*-rich and *trans–gauche* exchange conformations, respectively. These conformations are markedly different from *txtxtxtxt* and *xxxxxxxxx* in the corresponding components for the form α sample previously reported, probably reflecting the difference in crystallization from different nematic phases N_α and N_β. Moreover, molecular motion for the mesogen units and the spacer CH_2 sequences has been examined by the chemical shift anisotropy (CSA) analysis based on the magic angle turning (MAT) method. The mesogenic phenylene carbons are found to undergo rather restricted flip motion with amplitudes less than 30° around the bond axis in both crystalline and noncrystalline regions, while the flip rates associated with the ^{13}C spin–lattice relaxation may be greatly different in the two regions. The CSA spectrum of the spacer CH_2 carbons significantly narrows possibly as a result of the specific change in chain conformation in the crystalline and noncrystalline regions.

[DOI 10.1295/polymj.36.403]

KEY WORDS Liquid Crystalline Polymer / Polyether / Solid-State ^{13}C NMR / Liquid Crystalline Glass / Conformation / Co-planarity / Molecular Motion /

Recently we have successfully synthesized a new type of main-chain thermotropic liquid crystalline (LC) polyether (EDMB-10, Figure 1),[1] which is composed of 3,3′-dimethyl-4,4′-biphenyl units as mesogen and 10 methylene sequences as spacer, in a two-phase solvent system by using a phase transfer catalyst on the basis of syntheses of different LC polymers.[2–6] Since this LC polymer has rather low melting and isotropization temperatures around 120–130 °C, we could investigate the phase transition phenomena in detail without any chemical change during measurements.[7] By evaluating the results thus obtained, we have found that the LC glassy phase is readily produced by quenching the LC polymer from the melt to ice-water as a result of the suppression of crystallization after rapid liquid crystallization in this system.[8] Moreover, cold crystallization from the LC glassy phase is allowed to occur above the glass transition temperature, and another type of crystal form, form β, is produced, which is evidently different in wide-angle X-Ray diffraction profile from form α that is ordinarily crystallized by slowly cooling from the melt through the nematic phase. In particular, a form β sample with much higher crystallinity is obtained by annealing the LC glassy specimen at 130 °C for a certain period and then quenching it to 0 °C. This fact leads to an interesting proposal that another *stable* nematic phase may appear at about 130 °C on rapid heating from the LC glassy phase although the ordinary *unstable* nematic phase appearing on cooling from the melt is readily transformed to form α crystals without significant time delay in this system. The confirmation of the existence of such a stable nematic phase on heating will be made in near future by temperature-jump X-Ray diffractrometry.

In this paper, we characterize the structure and dynamics of the form β sample with high crystallinity newly crystallized from the LC glassy phase probably through the stable nematic phase described above by solid-state ^{13}C NMR spectroscopy. Especially the chain conformation and molecular motion of the spacer CH_2 sequences and mesogen groups are clarified separately in the crystalline and noncrystalline regions by comparing them with the corresponding re-

†To whom correspondence should be addressed (E-mail: horii@scl.kyoto-u.ac.jp).

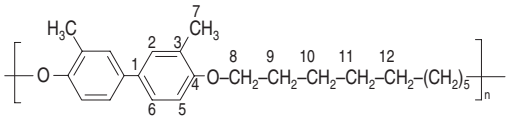

EDMB-10

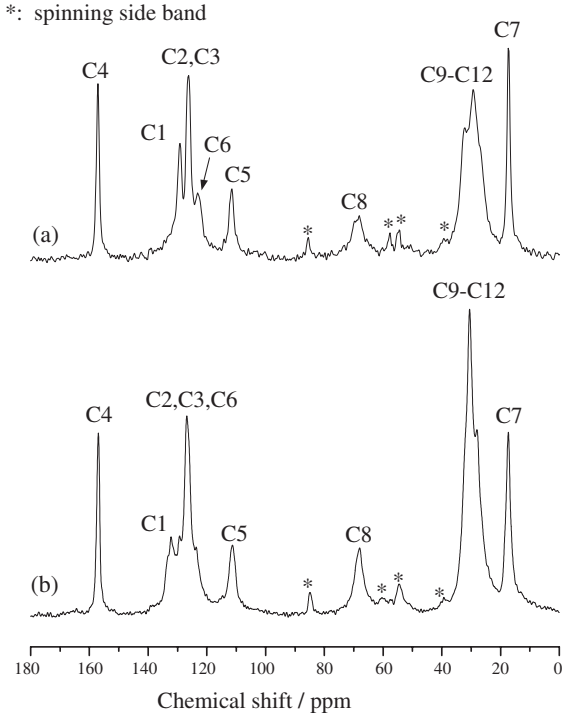

Figure 1. CP/MAS ^{13}C NMR spectra measured at room temperature. (a) the form α sample,[1] (b) the form β sample.

sults previously obtained for the form α sample.[1] A wide-angle X-Ray diffraction analysis of the crystal structure for forms α and β is in progress by using uniaxially oriented samples.[9]

EXPERIMENTAL

Sample

LC polyether EDMB-10 was synthesized by polymerizing 3,3′-dimethyl-4,4′-dihydroxy-biphenyl and 1,10-dibromodecane in a two phase system using a phase transfer catalyst as previously described in detail.[1] M_n of the sample thus obtained was determined to be 13,000 by polystyrene-calibrated GPC. The sample was brought to the LC glassy state by quenching from the melt to ice-water and then the form β sample was obtained by annealing the quenched sample at 130 °C for 30 min in a silicone bath and rapidly quenching to ice-water.[8]

Solid-State ^{13}C NMR Measurements

Solid-state ^{13}C NMR measurements were mainly performed at room temperature on a Chemagnetics CMX-200 spectrometer equipped with a JEOL solid-state NMR system operating at 50.0 MHz under a static magnetic field of 4.7 T.[1,7,10–13] ^{1}H and ^{13}C radio-frequency fields $\gamma B_1/2\pi$ were 62.5 kHz in the cross polarization (CP) process and the ^{1}H decoupling field strength was reduced by about 10%. The contact time for the CP process was 1 ms and the recycle time after the acquisition of a free induction decay (FID) was 5 s throughout this work. The MAS rate was set to 3.8 kHz to avoid the overlapping of spinning sidebands on other resonance lines. ^{13}C chemical shifts were expressed as values relative to tetramethylsilane (Me_4Si) by using the CH_3 line at 17.36 ppm of hexamethylbenzene crystals as an external reference. ^{13}C spin–lattice relaxation times (T_{1C}) were measured by using the CPT1 pulse sequence.[14]

2D magic angle turning (MAT) experiments[15,16] were conducted at room temperature on a Chemagnetics CMX-400 spectrometer operating under a static magnetic field of 9.4 T. The ^{1}H and ^{13}C radio-frequency field strengths $\gamma B_1/2\pi$ of 62.5 kHz, CP contact time of 2 ms, acquisition time of 2.56 ms, dwell time of 10 μs, and recycle time of 4 s were employed. The triple-echo sheared MAT pulse sequence[16] was used in this work by setting the τ delay to 20 μs. In the t_1 dimension, 64 slices with the increment of 30 μs were acquired. The MAS rate was precisely adjusted to 129 ± 1 Hz.

RESULTS AND DISCUSSION

CP/MAS ^{13}C NMR Spectra

Figure 1 shows CP/MAS ^{13}C NMR spectra observed at room temperature for the form α and form β samples of EDMB-10. Here, the spectrum of the form α sample is the same as previously reported.[1] As will be described later, both spectra contain the crystalline and noncrystalline components and, therefore, most assignments of the resonance lines are simply made for the isolated lines here. Interestingly, the line shapes for the C9–C12 carbons are found to appreciably differ between these two samples, suggesting different spacer conformations in the form α and form β crystals. In addition, somewhat different chemical shifts for the C1 and C6 carbons in the mesogen groups also imply that there may be some difference in co-planarity of the phenylene rings in the mesogen unit. In order to separate the crystalline and noncrystalline contributions, the T_{1C} relaxation process has been measured by the CPT1 pulse sequence.[14]

^{13}C Spin–Lattice Relaxation Behavior

The ^{13}C spin–lattice relaxation process for the form β sample has been measured at room temperature in a

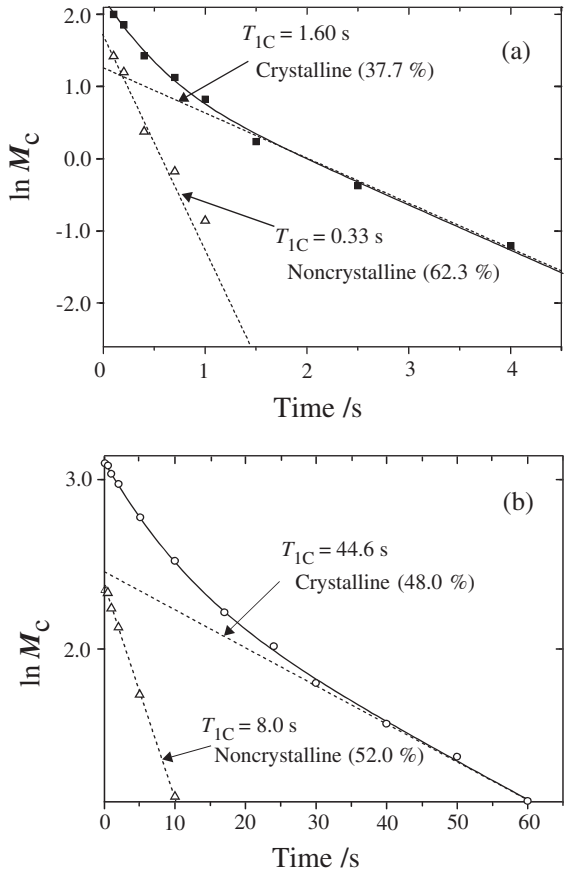

Figure 2. ^{13}C spin–lattice relaxation processes for the spacer and mesogen carbons measured at room temperature by the CPT1 sequence. (a) C9–C12 lines at about 30 ppm, (b) C4 line at 157 ppm.

similar way to the case of the form α sample[1] by using the CPT1 pulse sequence.[14] In Figure 2, the logarithmic peak intensity for the C9–C12 resonance lines at about 30 ppm or for the C4 line is plotted against the T_{1C} relaxation decay time. As is clearly seen in this figure, the respective decay curves can be simply described in terms of two components having different T_{1C} values which are denoted by broken lines. For reference, percentages of the respective components determined by the T_{1C} analyses are also given although the values are not so reliable mainly because of the difference in CP efficiency between the crystalline and noncrystalline components. Under this experimental condition, the longer T_{1C} component should be assigned to the crystalline component corresponding to form β crystals, while the shorter T_{1C} component is ascribed to the noncrystalline component that may be also called as the supercooled LC component. In contrast, the decay curve of the corresponding CH_2 carbons for the form α sample was composed of three components with different T_{1C} values, which were referred to as the crystalline (form α), medium, and noncrystalline (supercooled LC) components.[1] The cause of the disappearance of the medium component in the form β sample is not clear at present but the similarity of the structure in the crystalline and noncrystalline regions for this sample, which will be described later in detail, may be associated with its disappearance.

The T_{1C} values obtained for the isolated resonance lines of the form β sample by the decay curve analysis are summarized in Table I together with the corresponding results for the form α sample. The T_{1C} values of the mesogen groups for form β crystals are found to be significantly longer than those for form α crystals, indicating less molecular mobility of the mesogen groups in the former crystals. In contrast, the inner CH_2 carbons of the spacer sequence seem to have shorter T_{1C}s for form β than for form α, implying that the spacer CH_2 sequence may undergo more enhanced molecular motion in the form β crystals. Such different molecular mobility will be interpreted in relation to the conformation or packing of the respective structural units.

Crystalline and Noncrystalline Components

By using the difference in T_{1C}, the CP/MAS ^{13}C NMR spectra of the crystalline and noncrystalline components have been separately recorded for the form β sample in a similar way to the case of the form α sample.[1] Figure 3 shows the respective spectra of the inner CH_2 carbons of the spacer groups, together

Table I. ^{13}C Spin–Lattice Relaxation Times (T_{1C}) of the Mesogen and Spacer Carbons in the Respective Components at Room Temperature for the Form α and Form β Samples

Component	T_{1C}/s				
	Mesogen			Spacer	
	C4	C5	C7	C8	C9–C12
Form β					
Crystalline	44.6	32.0	18.0	7.00	1.60
Noncrystalline	8.0	2.3	3.5	1.19	0.33
Form α					
Crystalline	30.2	12.3	13.8	5.16	3.72
Medium				0.94	0.92
Noncrystalline	7.5	3.0	3.8	0.39	0.24

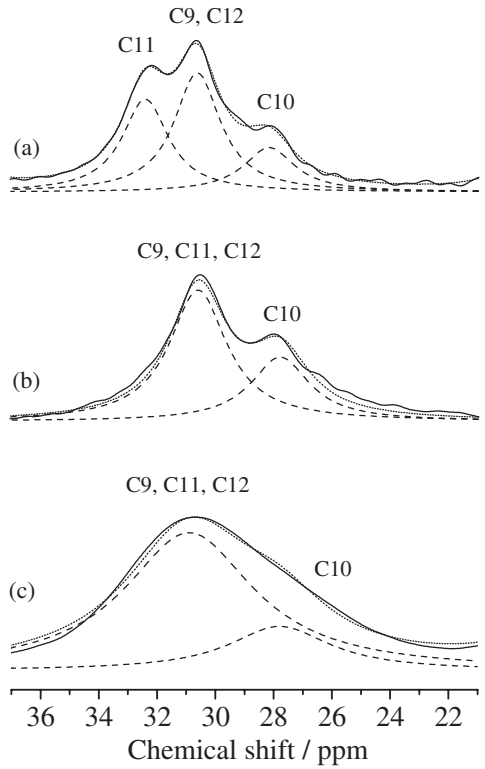

Figure 3. CP/MAS ^{13}C NMR spectra of different components for the form β sample in the CH_2 carbon region. (a) crystalline, (b) noncrystalline, (c) liquid crystalline glassy.[8] The broken lines indicate the results of the line shape analysis carried out by assuming that each constituent line is described as a Lorentzian.

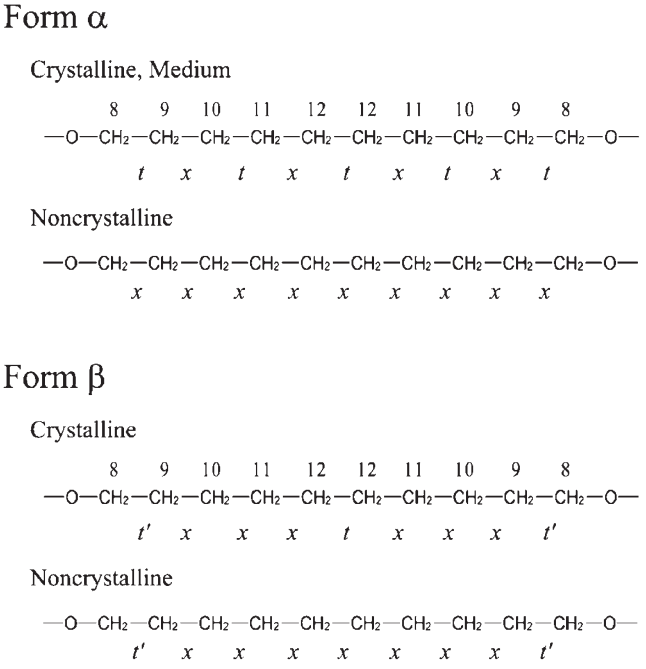

Figure 4. Chain conformation of the spacer CH_2 sequence for each component in the form α and β samples. t, t', and x indicate the *trans*, *trans*-rich, and *trans–gauche* exchange conformations, respectively.

with the corresponding spectrum of this polymer in the LC glassy state[8] measured at $-50\,^{\circ}C$ for comparison. The C8 resonance lines are not shown in this figure because there are no significant differences between two components. Here, the spectrum of the crystalline component was selectively measured as the longer T_{1C} component by the CPT1 pulse sequence[14] with a delay time τ of 2 s, while the noncrystalline spectrum was obtained by subtracting the crystalline spectrum from the spectrum obtained by the CPT1 pulse sequence with $\tau = 0.1$ s. It should be additionally noted that the relative intensities of the resonance lines thus obtained are not exactly proportional to the compositional ratios of the respective carbons because of their differences in T_{1C}.

These spectra have successfully been resolved into the respective constituent lines indicated by broken lines as shown in Figure 3 by assuming each line as a Lorentzian curve. As for the noncrystalline component, it is found that the spectrum is composed of two resonance lines at 27.8 and 30.6 ppm. These chemical shift values are very close to 26.7 ppm of the C10 line and 30.0 ppm of the C9, 11, 12 lines for the noncrystalline component in the form α sample,[1] respectively. It should be noted here that the assignment of the latter noncrystalline component was unambiguously made in the same way as in the isotopic melt because the chemical shifts are in good accord with those in the isotropic melt.[1] Accordingly, the lines at 27.8 and 30.6 ppm for the noncrystalline component in the form β sample should be also assigned to the C10 and C9, 11, 12 carbons, respectively, as shown in Figure 3b. Nevertheless, the C10 resonance line really shifts 1.1 ppm downfield for this component compared to the corresponding line in the form α sample. As previously reported,[1,7] each C–C bond in the spacer CH_2 sequence adopts the *trans–gauche* exchange conformation (x) in the noncrystalline component of the form α sample like at the isotropic melt. Such a downfield shift should, therefore, indicate that the C8–C9 bond associated with the C10 chemical shift will have the *trans*-rich conformation, which is denoted as t hereafter, in the noncrystalline region of the form β sample as a result of the decrease in the *γ-gauche* effect,[17] as shown in Figure 4. The ^{13}C chemical shift values thus obtained are listed in Table II together with the corresponding values for the form α sample and in the melt.

Interestingly, the line shape for the LC glassy phase is found to be almost the same as for the noncrystalline component of the form β sample as shown in Figure 3c and 3b, although the line width of each constituent line is much broader than that for the noncrystalline component. This fact suggests that the spacer conformation in the LC glassy phase may be nearly the same as in the noncrystalline component.

Table II. ^{13}C Isotropic Chemical Shift Values (δ_{iso}) of the Spacer and Mesogen Carbons Obtained by the Lineshape Analysis for the Respective Components of the form α and form β samples

Carbon	δ_{iso}/ppm				
	Crystalline		Noncrystalline		Melt
	Form α	Form β	Form α	Form β	
Spacer					
C8	68.2 (−0.9)	68.2 (−0.9)	67.5 (−1.6)	68.2 (−0.9)	69.1
C9	32.3 (+2.4)	30.6 (+0.7)	30.0 (+0.1)	30.6 (+0.7)	29.9
C10	28.6 (+2.0)	28.1 (+1.5)	26.7 (+0.1)	27.8 (+1.2)	26.6
C11	32.3 (+2.4)	32.4 (+2.5)	30.0 (+0.1)	30.6 (+0.7)	29.9
C12	32.3 (+2.4)	30.6 (+0.7)	30.0 (+0.1)	30.6 (+0.7)	29.9
Mesogen					
C1	128.3 (−5.6)	132.0 (−1.9)	132.5 (−1.4)	132.4 (−1.5)	133.9
C2	125.5 (−3.7)	126.7 (−2.5)	128.5 (−0.7)	126.4 (−2.8)	129.2
C3	125.5 (−1.9)	126.7 (−0.7)	125.8 (−1.6)	126.4 (−1.0)	127.4
C4	156.2 (−0.8)	157.0 (0)	156.7 (−0.3)	157.0 (0)	157.0
C5	111.0 (−1.7)	111.3 (−1.4)	111.1 (−1.6)	111.2 (−0.5)	112.7
C6	122.1 (−3.1)	126.7 (+1.5)	123.1 (−2.1)	126.4 (+1.2)	125.2

Values in parentheses for the respective carbons in each sample are the differences in chemical shifts between each component and the melt.

In contrast, an additional downfield line appears at 32.4 ppm for the crystalline component of the form β sample as evidently seen in Figure 3a. Other two constituent lines at 28.1 and 30.6 ppm for this component are found to have almost the same chemical shifts as those of the C10 and C9, 11, 12 lines for the noncrystalline component, respectively. Therefore, the most upfield line at 28.1 ppm should be straightforwardly assigned to the C10 carbon, but the assignment of other two lines will be made by considering the *γ-gauche* effect[17] as follows: The additional downfield line clearly shifts 1.8 ppm downfield compared to the resonance line of the C9, 11, 12 carbons of the noncrystalline component or 2.4 ppm downfield compared to the corresponding line of the noncrystalline component in the form α sample. This fact suggests that a certain C–C bond may adopt the *trans* conformation (*t*) in the crystalline component while this bond has the *trans–gauche* exchange conformation (*x*) in the noncrystalline component. The reason is that the conformational change from *x* to *t* will induce about 2–2.5 ppm downfield shift for only one carbon of the C9, 11, 12 carbons as a result of half of the *γ-gauche* effect. It is, therefore, concluded that the C12–C12 bond is allowed to have the *trans* conformation because this bond adopting *trans* induces the downfield shift only for the C11 carbon. If *trans* would be introduced for one bond of other C–C bonds, two CH_2 carbons might be subjected to the about 2–2.5 ppm downfield shift. However, this is not the case shown in Figure 3a. The assignment, ^{13}C chemical shift values, and the spacer conformation thus determined for the crystalline component are shown in Figure 3a, Table II, and Figure 4, respectively. For comparison, the spacer conformation of each component in the form α sample is also shown in Figure 4.

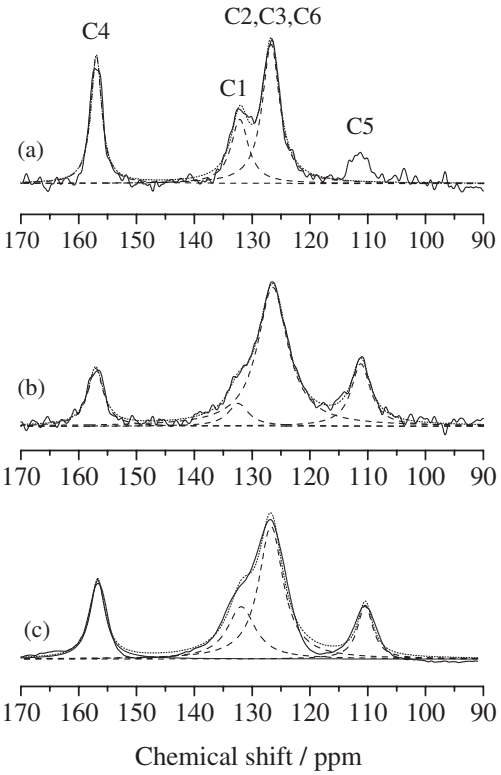

Figure 5. CP/MAS ^{13}C NMR spectra of different components for the form β sample in the mesogen carbon region. (a) crystalline, (b) noncrystalline, (c) liquid crystalline glassy.[8] Broken lines indicate the results of the line shape analysis carried out by assuming that each constituent line is described as a Lorentzian.

Figure 5 shows the CP/MAS ^{13}C NMR spectra of the crystalline and noncrystalline components of the form β sample in the mesogen carbon region, which

were obtained in a similar way to the case shown in Figure 3. For comparison, the spectrum of EDMB-10 in the LC glassy state measured at 0 °C is also shown in this figure. It is found that the ^{13}C chemical shifts of the respective resonance lines in these three states are in good accord with each other within an experimental error. This fact indicates that the structure of the mesogen groups is almost the same in the three states. The ^{13}C chemical shift values of the mesogen carbons for the crystalline and noncrystalline components in the form α and β samples are also compiled in Table II. The values shown in parentheses for the respective carbons are the differences in chemical shifts between the crystalline (or noncrystalline) component in each sample and the melt. Most evident differences in parentheses are recognized for the mesogen carbons of the crystalline component of the form α sample and the values are remarkably decreased in the order of the C1, C2/C6, C3/C5, and C4 carbons. This fact suggests that the co-planarity of the adjacent phenylene rings in the mesogen group may be greatly different in the crystalline component of the form α sample from that in the melt. In fact, more explicit dependences of the ^{13}C chemical shifts of the phenylene carbons on the torsion angles around the C–C bond connecting the adjacent phenylene groups were observed for low-molecular-weight model compounds and their theoretical supports were also obtained by quantum chemical calculations.[18] It is, therefore, concluded that the mesogen groups have a much higher level of co-planarity in the form α crystals compared to those in the melt.

In contrast, the corresponding values in parentheses for the crystalline component of the form β sample is appreciably smaller compared to the cases for the form α sample. This fact indicates a lower level of the co-planarity of the mesogen groups in the form β crystals than in the form α crystals. The detailed difference in co-planarity between the two crystal forms will be revealed by the WAXS crystal structure analysis which is now in progress.[9] It should be here noted that there are also significant differences in parentheses for the mesogen carbons of the noncrystalline components in the two samples: The co-planarity of the mesogen groups may be almost the same level for the noncrystalline component in the form β sample as that for the form β crystals because the values in parentheses are nearly the same for the respective carbons in these two components. However, it seems difficult to estimate the level of the co-planarity for the noncrystalline component in the form α sample because the values in parentheses are irregularly dispersed unlike the case of the crystalline component in this sample and seems not to be interpreted only in terms of the co-planarity. Some kind of molecular motion or intermolecular interaction may make the effect of the co-planarity obscure in this noncrystalline region. Nevertheless, it should be pointed out that the structure of the mesogen groups is also significantly different between the two noncrystalline components included in the form α and β samples similarly to the conformational differences in the spacer CH_2 sequences as shown in Figure 4. Moreover, the mesogen groups in the noncrystalline region of the form α sample should have the structure significantly different from that in the melt which will be preferable for the formation of the LC phase, although the spacer CH_2 sequence adopts almost the same conformation as that in the melt as described above.

Such findings are very important to support our recent proposal that there exist two nematic phases, N_α and N_β, from which form α and β crystals are crystallized in the EDMB-10 system, respectively.[8] Since the noncrystalline component corresponds to the supercooled LC component in each sample crystallized from the LC phase, the structure of the mesogen and spacer groups in the LC phase may be preserved in the supercooled LC component which is left without crystallization in each sample. Therefore, the N_α and N_β phases must have also different structures in the mesogen and spacer units as described above for the supercooled noncrystalline components in the form α and β samples.

Molecular Motion of the Mesogen and Spacer Groups

As already described, the T_{1C} values of the mesogen carbons given in Table I indicate that molecular motion with a correlation time of the order of 10^{-8} s responsible for the T_{1C} relaxation is somewhat more restricted in the form β crystals than in the form α crystals. However, there is no significant difference in molecular mobility in the noncrystalline region between the form α and form β samples, although the mesogen groups are subjected to much more enhanced motion in this region compared to those in the crystalline region. To examine the molecular motion of the mesogen units in more detail, ^{13}C CSA spectra of the respective carbons have been measured for the form β sample in a similar way to the case of the form α sample[7] by 2D MAT ^{13}C NMR spectroscopy.[15,16]

Figure 6 shows the 2D MAT ^{13}C NMR spectrum of the form β sample obtained at room temperature under an ultra-slow MAS condition. The "sky projection" plots of the highest points in each column and row of the 2D spectrum are also shown in the F_1 and F_2 dimensions, respectively. The projection spectrum shown in the F_1 dimension is a high resolution spectrum which is equivalent to the CP/MAS spectrum shown in Figure 1b but side-band free. The CSA spectra seem to be well separately obtained along the F_2

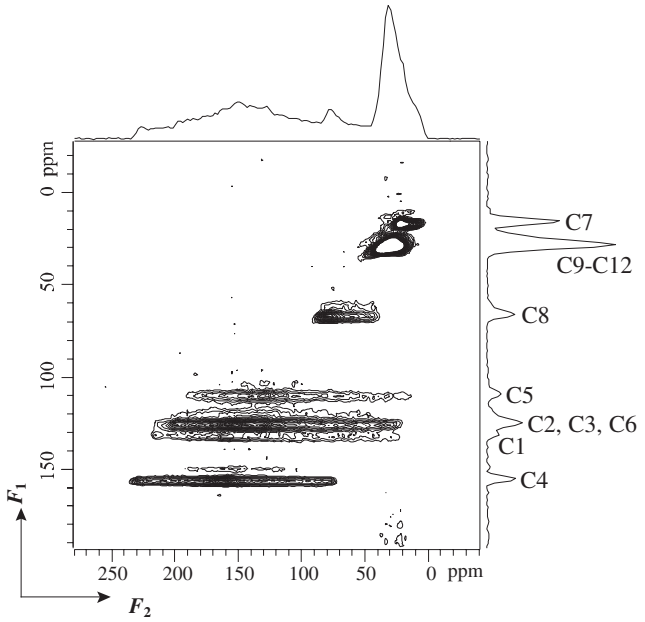

Figure 6. 2D MAT ^{13}C NMR spectrum measured at room temperature for the form β sample.

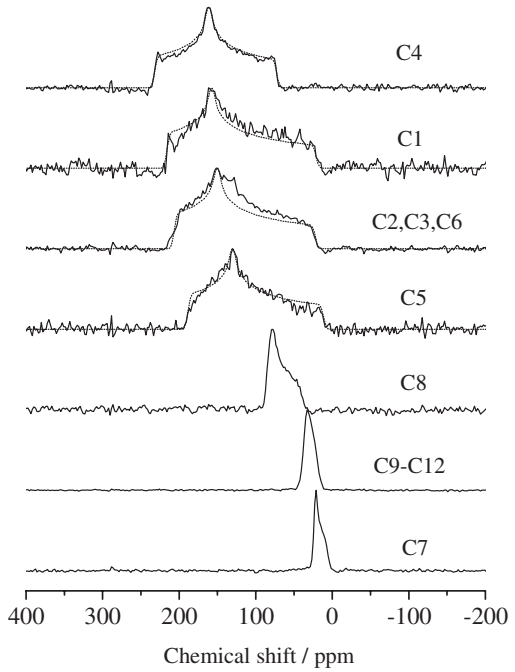

Figure 7. ^{13}C CSA spectra for different carbons in the form β sample, which were obtained as slices along the F_2 axis in the 2D MAT spectrum shown in Figure 6. Dotted lines are the CSA powder patterns simulated for the respective carbons in the rigid state.

axis in the 2D spectrum for the respective resonance lines of the high resolution projection spectrum shown at the right side in this figure.

In Figure 7, the CSA spectra thus obtained as slices along the F_2 axis are shown for the respective carbons. In this sample, the CSA spectra are also found to be successfully measured by the 2D MAT method similarly to the cases of the form α sample.[7] For the mesogen carbons, the simulated CSA spectra in the rigid state are also shown as dotted lines. Except for the case of the overlapped C2, C3, C6 CSA spectra, the observed CSA spectra are in good accord with the simulated spectra for the C4, C1, and C5 carbons. The principal values σ_{11}, σ_{22}, σ_{33} used in the CSA simulations are compiled in Table III. The corresponding values of the form α sample,[7] dimethoxy benzene (DMB) and diethoxy benzene (DEB) crystals[19] are also given for comparison. The chemical shift anisotropy $|\sigma_{11} - \sigma_{33}|$ of the aromatic CH carbon for the form β sample seems not to be much different from the values for the DMB and DEB crystals. This fact suggests that the phenylene rings in the mesogen units may be highly hindered in molecular motion in the noncrystalline component as well as in the crystalline component although these two components are superposed in the CSA spectra. As is already described above, however, there are marked difference in T_{1C} between the crystalline and noncrystalline components.

To interpret the CSA and T_{1C} results that seem to be in conflict with each other, the change in CSA line shape has been simulated for the phenylene flip motion around the bond axis as a function of flip angle by assuming the two-site exchange model.[20,21] Figure 8 shows the CSA spectra thus simulated for the aromatic CH carbon (C5) under the fast limit condition for different flip angles. Here, the principal values experimentally obtained for the C5 carbon in Table III were used. As clearly seen in this figure, the CSA line shape and the anisotropy $|\sigma_{11} - \sigma_{33}|$ for a flip angle of 30° do not appreciably change from those in the static state. This fact implies that the phenylene rings in the mesogen groups may be subjected to the rapid random fluctuation around the bond axis with the flip angles less than 30° in the noncrystalline region and such motion will induce rather fast T_{1C} relaxation without significant change in CSA for the C5 carbon. Even in the crystalline region, similar fluctuation of the phenylene rings may be allowable although the flip frequencies will be much reduced resulting in the increase in T_{1C}. Recent ^{13}C CSA quantum chemical calculations combined with CSA measurements[22] also support the occurrence of somewhat enhanced molecular motion for phenylene or benzene rings in solid samples; it was pointed out that benzene rings of biphenyl may preferably undergo both internal jumping between slightly different enantiomeric structures and overall molecular librations with an angle of ±12° in the crystalline state. Such rapid fluctuation of the phenylene groups in the LC polymer samples may also enable the methylene sequences to undergo much higher molecular mobility and then to

Table III. Principal Values of ^{13}C Chemical Shift Tensors for the Mesogen Carbons Obtained for the Form α and Form β Samples by the 2D MAT Experiment

Sample	Carbon	Chemical shift/ppm				
		σ_{11}	σ_{22}	σ_{33}	$\lvert\sigma_{11}-\sigma_{33}\rvert$	σ_{iso}[a]
form β	C1 (qC[b])	217	158	22	195	132
	C4 (qC)	233	162	73	160	157
	C5 (CH)	189	131	12	177	112
form α	C1 (qC)[c]	—	—	—	—	129
	C4 (qC)	224	164	78	146	156
	C5 (CH)	187	131	19	168	112
DMB[d]	qC	243	160	71	172	158
	CH	199	137	22	177	119
	CH	194	131	13	181	113
DEB[e]	qC	233	160	71	162	155
	CH	199	135	24	175	119
	CH	194	129	11	183	111

[a]determined by the MAS experment for the form α and β samples. For DMB and DEB, σ_{iso} is calculated from the principal values. [b]qC denotes a quaternary carbon. [c]not ressolved well in the 2D MAT spectrum. [d]dimethoxy benzene (Ref 19). [e]diethoxy benzene (Ref 19).

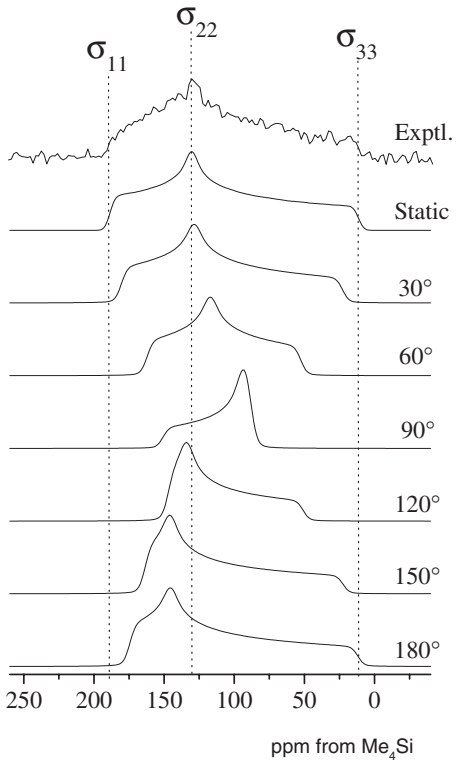

Figure 8. CSA powder patterns simulated for the aromatic CH (C5) carbon by assuming two-site flip motion of the phenylene ring around the bond axis with different flip angles under the fast limit condition.

adopt the specific conformation shown in Figure 4 even in the crystalline region.

The slice CSA spectra of the C8 (OCH_2) and C7 (CH_3) carbons shown in Figure 7 seem to be axially symmetric like the case of the form α sample and their chemical shift anisotropies $|\sigma_{11}-\sigma_{33}|$ are also of the same orders for the corresponding carbons in the form α sample.[7] As described previously,[7] the σ_{11} and σ_{22} values of the OCH_2 carbons in the rigid state are equal for poly(ethylene terephthalate)[19,23] or not so greatly different from each other for poly(ethylene oxide).[19,24] It is, therefore, difficult to obtain any information of the molecular motion of the OCH_2 carbons from the CSA line shape. In contrast, the CSA spectra of the rigid CH_3 carbons have a typical powder pattern with different principal values for toluene[19,25] and *p*-xylene.[19,26] Therefore, the axially symmetric CSA spectrum of the C7 carbons clearly indicates the rapid rotation of the CH_3 groups even in the crystalline region. Moreover, the $|\sigma_{11}-\sigma_{33}|$ value for the C7 carbon is much reduced to about 14 ppm compared to the values (22.5, 26.5 ppm) obtained for toluene and *p*-xylene[19] by assuming a simple rotation of the CH_3 group. This fact implies that the phenylene rings connecting the CH_3 groups may undergo thermal fluctuation with small amplitudes around the virtual C1–C4 bond, in good accord with the result described above for the CSA of the aromatic CH carbons, and contribute to narrowing of the CSA spectrum of the CH_3 carbons.

The CSA spectrum of the C9–C12 carbons in the spacer unit shown in Figure 7, which was obtained as a slice along the F_2 axis at 30.6 ppm in Figure 6, seems to narrow to a considerable extent reflecting the higher molecular mobility of the CH_2 sequences. Figure 9 shows the enlarged CSA spectrum of the CH_2 carbons together with the CSA powder spectrum having the same isotropic chemical shift for the CH_2 carbon in the rigid state. The latter spectrum was simulated by using the principal values for polyethylene crystals.[19,27] Although the observed CSA spectrum

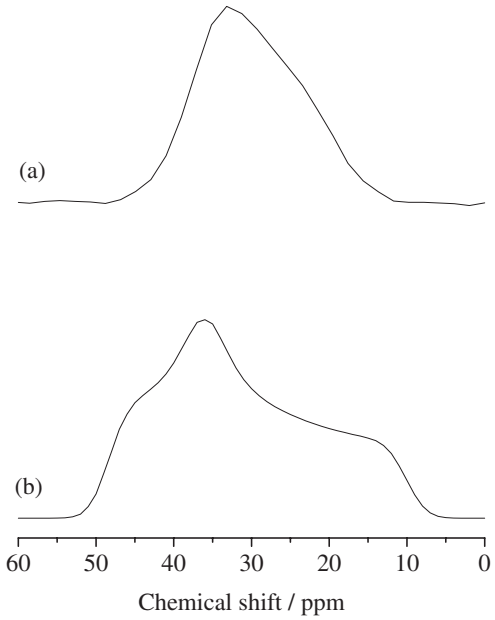

Figure 9. (a) Enlarged CSA spectrum of the C9–C12 carbons which is originally shown in Figure 7. (b) CSA powder spectrum for polyethylene crystals with an isotropic chemical shift value of 30.6 ppm.[27]

contains the contributions from several constituent CH_2 carbons, the overall spectrum is found to narrow to a remarkable extent. Such narrowing should be the reflection of the specific *trans–gauche* exchange conformation of the CH_2 sequences in the crystalline region shown in Figure 4. Moreover, the CSA line shape of the noncrystalline component may be not significantly different from the overall CSA spectrum in Figure 9, because this contribution is also involved in this spectrum. This fact suggests that each *trans–gauche* exchange motion may be not independently induced possibly unlike in the melt and some kind of cooperative motion will be allowable under the restriction of the oriented mesogen groups in the noncrystalline component which corresponds to the supercooled LC component. Further characterization of the chain conformation and dynamics will be performed in the *stable* nematic phase after the confirmation of the existence of the phase by temperature-jump X-Ray diffractometry.

CONCLUSIONS

We have characterized in detail the structure and chain conformation for the form β sample of a new type of thermotropic LC polyether (EDMB-10), which was crystallized from the LC glassy phase, by solid-state ^{13}C NMR spectroscopy and obtained the following conclusions:

(1) CP/MAS ^{13}C NMR spectrum of the form β sample suggests that the chain conformation of the spacer CH_2 sequences and mesogen groups in this sample may be significantly different from those previously reported for the form α sample that was crystallized by slowly cooling from the melt through the nematic phase. To confirm such a suggestion, ^{13}C spin–lattice relaxation behavior has been examined in detail and the spectra of the crystalline and noncrystalline components have been separately obtained by using their difference in T_{1C}.

(2) The evaluation of the ^{13}C chemical shift values of the spacer CH_2 carbons in the respective spectra mainly by the γ-*gauche* effect reveals that the CH_2 sequences adopt the $t'xxxtxxxt'$ conformation in the crystalline region while their preferable conformation is $t'xxxxxxxt'$ in the noncrystalline region. Here, t, t', and x are the *trans*, *trans*-rich, and *trans–gauche* exchange conformation. These conformations are appreciably different from *txtxtxtxt* in the crystalline region and *xxxxxxxxx* in the noncrystalline region for the form α sample previously reported, probably reflecting the structure difference in the nematic phases, N_α and N_β, from which forms α and β are crystallized, respectively.

(3) By the comparison of the ^{13}C chemical shifts of the mesogenic phenylene carbons in the crystalline and noncrystalline components with those in the melt, it is found that the co-planarity of the adjacent phenylene groups in the mesogen units is of a much higher level in form α crystals compared to that for form β crystals. Moreover, the structure of the mesogen groups is also significantly different in the noncrystalline region between the form α and β samples, also reflecting the differences in structure in the N_α and N_β phases.

(4) The chemical shift anisotropy (CSA) spectra for the respective carbons in the form β sample have been obtained by the 2D MAT method. The analysis in terms of the two-site exchange model for the CSA spectrum thus obtained for the aromatic CH carbons reveals that the phenylene groups undergo rapid fluctuation around the bond axis with amplitudes less than 30° in the crystalline and noncrystalline regions although the fluctuation rates that may be reflected to the ^{13}C spin–lattice relaxations are greatly different in the crystalline and noncrystalline regions. On the other hand, the CSA spectrum of the inner CH_2 carbons significantly narrows in the crystalline and noncrystalline regions, indicating the rapid specific change in conformation in the respective regions.

Acknowledgment. This work was supported by a Grant-in-Aid for Scientific Research (No. 12450384) from the Ministry of Education, Culture, Sports, Science and Technology, Japan.

REFERENCES

1. H. Ishida and F. Horii, *Macromolecules*, **34**, 7751 (2001).
2. "Liquid Crystallinity in Polymers. Principles and Fundamental Properties," A. Ciferri, Ed., VCH Publishers, New York, N.Y., 1991.
3. "Liquid-Crystalline Polymer Systems. Technological Advances," A. I. Isayev, T. Kyu, and S. Z. D. Cheng, Ed., ACS Symp. Series 632, Am. Chem. Soc., Washington, D.C., 1996.
4. "Handbook of Liquid Crystal Research," P. J. Collings and J. S. Patel, Ed., Oxford Univ. Press, New York, N.Y., 1997.
5. "Structure and Properties of Oriented Polymers," I. M. Ward, Ed., Chapman & Hall, London, 1997.
6. "Thermotropic Liquid Crystal Polymers," T.-S. Chung, Ed., Technomic, Lancaster, 2001.
7. M. Murakami, H. Ishida, M. Miyazaki, H. Kaji, and F. Horii, *Macromolecules*, **36**, 4160 (2003).
8. M. Murakami, H. Ishida, H. Kaji, and F. Horii, *Polym. J.*, **35**, 951 (2003).
9. M. Ooyama, T. Yamamoto, K. Nozaki, and F. Horii, *Polym. Prepr. Jpn.*, **52**, 549 (2003).
10. H. Ishida and F. Horii, *Macromolecules*, **35**, 5550 (2002).
11. Y. Ohira, F. Horii, and T. Nakaoki, *Macromolecules*, **34**, 1655 (2001).
12. K. Kuwabara, H. Kaji, M. Tsuji, and F. Horii, *Macromolecules*, **33**, 8520 (2000).
13. K. Masuda and F. Horii, *Macromolecules*, **31**, 5810 (1998).
14. Z. Gan, *J. Am. Chem. Soc.*, **114**, 8307 (1992).
15. J. Z. Hu, A. M. Orendt, D. W. R. J. P. Alderman, C. H. Ye, and D. M. Grant, *Solid State Nucl. Magn. Reson.*, **3**, 181 (1994).
16. D. A. Torchia, *J. Magn. Reson.*, **44**, 117 (1981).
17. A. E. Tonelli, "NMR Spectroscopy and Polymer Microstructure: The Conformational Connection," VCH Publishers, New York, N.Y., 1989.
18. S. Ando, T. Hironaka, H. Kurosu, and I. Ando, *Magn. Reson. Chem.*, **38**, 241 (2000).
19. T. M. Duncan, "A Compilation of Chemical Shift Anisotropies," Farragut Press, Chicago, IL, 1990.
20. M. Mehring, "Principles of High Resolution NMR in Solids," Springer-Verlag, Berlin, 1993.
21. F. Horii, *Bull. Inst. Chem. Res., Kyoto Univ.*, **70**, 198 (1992).
22. D. H. Barich, R. J. Pugmire, D. M. Grant, and R. J. Iuliucci, *J. Phys. Chem. A*, **105**, 6780 (2001).
23. P. B. Murphy, T. Taki, B. C. Gerstein, P. M. Henrichs, and D. J. Massa, *J. Magn. Reson.*, **49**, 99 (1982).
24. W. W. Fleming, C. A. Fyfe, R. D. Kendrick, J. R. Lyerla, H. Vanni, and C. S. Yannoni, "Polymer Characterization by ESR and NMR," A. E. Woodward and F. A. Bovey, Ed., ACS Symp. Ser. No. 142, 1980, p 193.
25. A. Pines, M. G. Gibby, and J. S. Waugh, *Chem. Phys. Lett.*, **15**, 373 (1972).
26. J. Van Dogen Torman and W. S. Veeman, *J. Chem. Phys.*, **68**, 3233 (1978).
27. D. L. VanderHart, *J. Chem. Phys.*, **64**, 830 (1976).